

Article

Removal Rates of NO_x, SO_x, and Fine Dust Particles in Textile Fabrics Coated with Zeolite and Coconut Shell Activated Carbon

Keun-Hyeok Yang ¹, Ju-Hyun Mun ^{1,*} and Jae-Uk Lee ²¹ Department of Architectural Engineering, Kyonggi University, Suwon 16227, Korea; yangkh@kgu.ac.kr² Department of Architectural Engineering, Graduate student, Kyonggi University, Suwon 16227, Korea; jlee940303@nate.com

* Correspondence: mjh@kgu.ac.kr; Tel.: +82-031-249-9715

Received: 13 October 2020; Accepted: 10 November 2020; Published: 12 November 2020



Abstract: An effective dipping method for coating of textile fabrics with porous materials is proposed on the basis of the use of epoxy solution consisted of resins, crosslinkers, and dilution solutions. The removal rates of nitrogen oxides (NO_x), sulfur oxides (SO_x), and fine dust particles in the coated textile fabrics are accessed. The textile fabrics made of polyester are used to effectively reduce fine dust particles through static electricity. Zeolite and coconut shell activated carbon are used as porous material to reduce SO_x and NO_x, respectively. The effects of the epoxy content and dilution solution types on the SO_x removal rate of textile fabrics coated with zeolite are evaluated to determine the optimum coating conditions. In addition, the effects of external environmental conditions, such as washing and freeze thawing, on the SO_x and NO_x removal rates of the textile fabrics coated with porous materials using the optimum coating conditions are examined. The test results show that the SO_x removal rate of textile fabrics coated with zeolite decreases with the increase in the epoxy content. The decrease is 2.9 times larger for textile fabrics coated using deionized water than those coated using isopropyl alcohol. After one wash, the SO_x removal rate decreases dramatically. However, the decrease is reduced by 16% when the epoxy content ratio is increased by 0.5%. The effects of washing and freeze thawing on the SO_x and NO_x removal rates of textile fabrics coated using the deionized water diluted with the epoxy content ratio of 2% are minimal. Consequently, to maintain stable SO_x and NO_x removal rates under external environmental conditions such as washing and freeze thawing, 98% deionized water dilution and 2% epoxy content ratio are required for the optimum coating of textile fabrics with zeolite and coconut shell activated carbon.

Keywords: textile fabric; zeolite; coconut shell activated carbon; NO_x; SO_x; fine dust particle

1. Introduction

In general, 60% of the fine dust in air is composed of the sulfates or nitrates produced by the combination of exhaust gases, such as sulfur oxides (SO_x) and nitrogen oxides (NO_x), with water vapor or ammonia in air [1,2]. Therefore, various efforts have been made to reduce the air pollutants that produce fine dust, particularly in the construction industry [3,4]. Trapalis et al. [3] developed a nanocomposite TiO₂ produced from the combination of pure TiO₂ and titanium isopropoxide, and showed that its efficiency in removing NO_x is better than that of pure TiO₂. Guo et al. [4] showed that a higher NO_x removal rate was exhibited in a concrete block coated with TiO₂ compared to that imbedded with TiO₂. However, most of the existing studies on the removal of air pollutants are based on chemical adsorption by the photocatalyst titanium dioxide (TiO₂). The adsorption efficiency of TiO₂ in external environmental conditions, such as washing and freeze thawing, is much lower because

TiO₂ is soluble in water [5]. In addition, the techniques applied in the construction industry have only focused on the removal of NO_x, whereas the removal of fine dust particles has received limited attention [6]. Hence, in the construction industry, the techniques for removing stable air pollutants and fine dust particles in external environments are required.

Textile fabrics made of polypropylene or polyester formed from fibers with various small diameters are commonly used in the construction industry. Static electricity can be effectively induced by friction in these textile fabrics through rubbing their surfaces. The static electricity can easily cause fine dust particles to adhere to the fabrics owing to the movement of charges. An [7] reported the adsorption of fine dust particles by static electricity in dried polyester fabrics. Kim et al. [8] reported that the fine dust particle removal rate in textile fabrics increased with the applied voltage. Meanwhile, zeolite has a large polarization and effectively forms covalent bonds with SO_x, which has dipole moments in ranges similar to that of zeolite [9,10]. Lee et al. [11] studied the reproducibility of the NO_x removal rate by zeolite and reported that the NO_x removal rate in zeolite was maintained above 90% throughout 27 times repeats of the experiment. Kopaç and Kocabaş [12] proposed a mechanism for the surface adsorption of SO₂ on zeolite.

The polarization of coconut shell activated carbon is relatively very low, and effectively forms covalent bonds with NO_x, which has dipole moments in similar ranges to that in coconut shell activated carbon [9,13]. In addition, coconut shell activated carbon can physically adsorb NO_x because its pore size is similar to the movement range of the NO_x gas molecules [14]. Park et al. [15] reported that the NO_x removal rate of coconut shell activated carbon was improved by 40% after plating the surface of the coconut shell activated carbon with Cu. Lee et al. [16] showed that coconut shell activated carbon with more micropores exhibited a higher NO_x removal rate. These results imply that the combination of textile fibers and zeolite or coconut shell activated carbon could be very effective in reducing air pollutants and fine dust particles. Hence, a coating method for textile fibers that maintains a stable air pollutant and fine dust particle removal rate in external environments is required.

The objective of this study is to propose an effective coating method for textile fabrics and evaluate the removal rates of nitrogen oxides (NO_x), sulfur oxides (SO_x), and fine dust particle in the coated textile fabrics. To effectively reduce the fine dust particles using static electricity, textile fibers made of polyester were used. Zeolite and coconut shell activated carbon were used as porous materials to remove SO_x and NO_x, respectively. In the coating process, the textile fibers were dipped into a solution of epoxy diluted with deionized water or isopropyl alcohol and combined with the porous materials by a mixer. The effects of the length and density of the uncoated textile fabrics on the removal of fine dust particles were evaluated. In the textile fabrics coated with zeolite, the effects of the epoxy content and the dilution solution type on the SO_x removal rate were evaluated and the optimum coating conditions were determined based on these results. In addition, the SO_x and NO_x removal rates of textile fabrics respectively coated with zeolite and coconut shell activated carbon, using the determined optimum coating conditions were evaluated after washing and freeze thawing to ascertain the removal of stable air pollutants in external environments. Based on the findings obtained by this study, the new textile fibers are proposed for building materials that are capable of reducing NO_x, SO_x, and fine dust particles based on adsorption mechanisms without any electric power consumption.

2. Materials and Methods

2.1. Material

Table 1 summarizes the physical properties of the porous materials used. The textile fabrics were made of polyester, and their length and fiber diameter were 15 mm and 20 μm, respectively. The zeolite was compiled from a crystalline alkali aluminosilicate mineral (1318-02-1, Sigma-Aldrich, Inc., St. Louis, MO, USA). The sizes of the zeolite particles ranged between 3 and 10 μm, resulting in a typical pore size of approximately 4 Angstroms. The density of the zeolite particles was 2.37 g/cm³. The coconut shell activated carbon was produced with the pelletized and impregnated activated

carbons (CDGA, Dongyang Co. Ltd., Cheonan, South Korea). The sizes of the coconut shell activated carbon particles were between 5 and 10 μm , and the density of the coconut shell activated carbon was 1.56 g/cm^3 . The epoxy used for adhesive was made of a cold mounting resin and crosslinker (West System, Gougeon Brothers, Inc., Bay City, MI, USA), which can be hardened within 12 h at the hardness of 83 Shore D. The density of hardened epoxy was 1.18 g/cm^3 . The temperature rise during the cross-linking did not exceed 50 $^\circ\text{C}$.

Table 1. Physical properties of porous materials.

Type	Particle Size (μm)	Density (g/cm^3)	Fineness (m^2/g)
Zeolite	3–10	2.37	2.3
Coconut shell activated carbon	5–10	1.56	1130.1

Figure 1 shows the distributions of the pore sizes and images of the internal pores in the porous materials. Pore sizes ranging between 0.4 and 185 nm were measured using the Brunauer–Emmett–Teller (BET) technique, while pore sizes larger than 185 nm were measured using mercury intrusion porosimetry. The internal microstructure was analyzed from the scanning electron microscopy (SEM) images. As shown in Figure 1a, the textile fibers had cylindrical shapes and were intertwined. The micropores, mesopores, and macropores respectively constituted 7.4%, 2.7%, and 89.9% of the pores in zeolite, indicating that most of the pores in zeolite were larger than 0.05 μm . As shown in Figure 1b, the internal structure of zeolite consisted of irregular polygons. The micropore, mesopore, and macropore distribution in coconut shell activated carbon were 74.7%, 9.7%, and 15.6%, respectively, indicating that the most common pore size in zeolite was the micropore, which is similar to the range of molecular movement in NO_x [14]. In addition, the internal structure of the coconut shell activated carbon had many pores of various diameters (Figure 1c). The micropore, mesopore, and macropore distribution of hardened epoxy were 15.0%, 2.7%, and 85.3%, respectively, indicating that the most common pore size in epoxy was the macropore, which was 5.7 times larger than the molecular movement range of SO_x and NO_x .

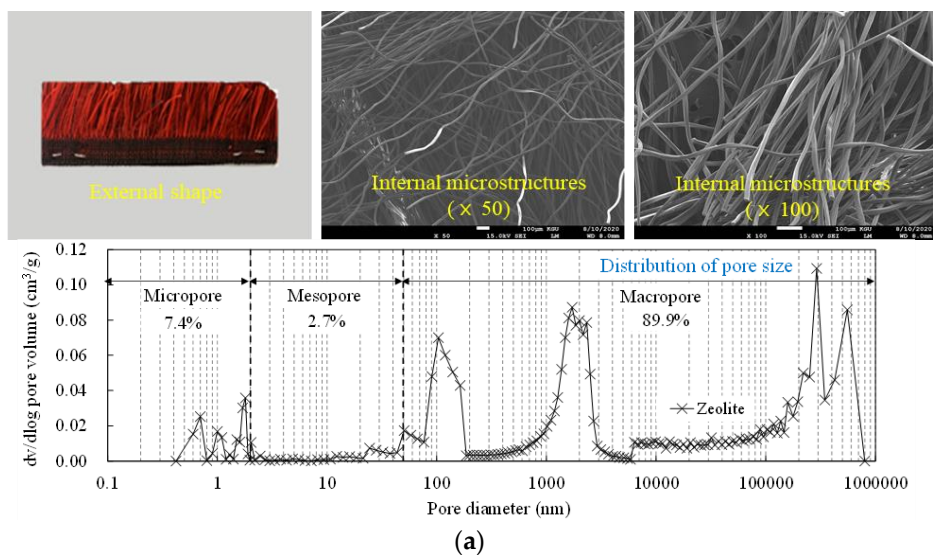


Figure 1. Cont.

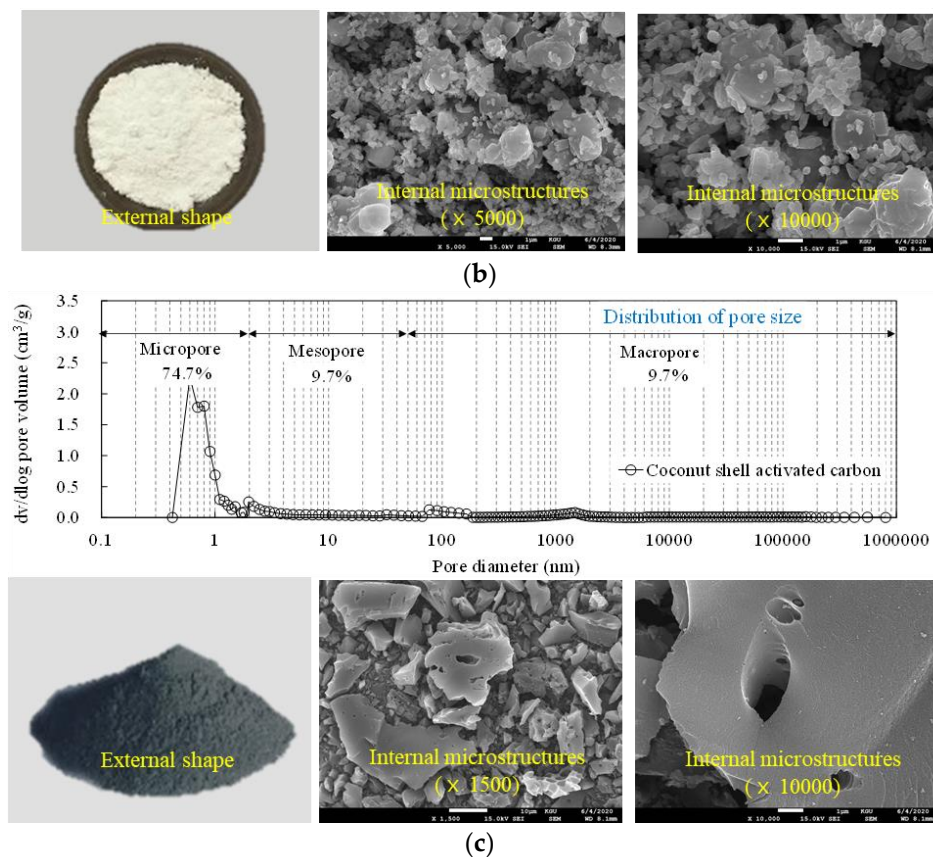


Figure 1. Internal microstructure and pore distribution of each material used. (a) Textile fabrics. (b) Zeolite. (c) Coconut shell activated carbon.

2.2. Methods

Tables 2 and 3 summarize the main parameters studied in the experiments. The adsorption of fine dust particles by static electricity was investigated in the uncoated textile fabrics. The length and number of layers of uncoated textile fabrics were selected as the main parameters. The length of the uncoated textile fabrics was set as 3.5, 7, or 12 mm, which correspond to the densities of 0.08 g/cm², 0.13 g/cm², and 0.22 g/cm², respectively. The number of layers was set as 4 or 8. Static electricity was introduced into all the textile fabrics artificially by rubbing their top surfaces. In the textile fabrics coated with zeolite, the epoxy content and dilution solution were selected as the main parameters. Additionally, the numbers of washings and freeze–thaw cycles were selected as the main parameters to consider the effects of rain and temperature in the external environment. Deionized water and isopropyl alcohol were used for the dilution solution. Based on the previous test results performed by Lim et al. [17], resins and crosslinkers were incorporated at a mass ratio of 4:1 and then used as an adhesive to enhance the effectiveness of the cross-linking. The ratio of the epoxy content in the diluted solution was varied from 0 to 2%. The number of washings was set to 0, 1, or 10, and the number of freeze–thaw cycles to 0 and 1 cycle. The number of washings and freeze–thaw cycles used for the textile fabrics coated with coconut shell activated carbon were identical to those selected for textile fabrics coated with zeolite. The optimum epoxy content and solution determined from the coating process of zeolite were used for the coating the textile fibers with coconut shell activated carbon.

Table 2. Main parameters for evaluating the fine dust particle removal rate of the textile fabric specimens.

Specimen	Length (mm)	Layers	Density (g/cm ²)	Details
C (Control)	-	-	-	
3.5-4	3.5	4	0.08	
3.5-8	3.5	8	0.08	
7.0-4	7	4	0.13	
7.0-8	7	8	0.13	
12-4	12	4	0.22	
12-8	12	8	0.22	

Note: the specimen notation includes two parts except for specimen C. The first and second parts indicate the length and number of layers of uncoated textile fabrics, respectively.

Table 3. Main parameters for evaluating the NO_x and SO_x removal rates of the textile fabric specimens.

Specimens	Porous Material Type	Dilution Solution Type	Epoxy Contents (%)	Number of Washings	Number of Freezing–Thaw Cycles
Z-D-C (Control)			0	0	0
Z-D-0-1				1	0
Z-D-1-0			1	0	0
Z-D-1-1				1	0
Z-D-1.5-0	Zeolite	Deionized water	1.5	0	0
Z-D-1.5-1				1	0
Z-D-2-0				0	0
Z-D-2-1				1	0
Z-D-2-10			2	10	0
Z-D-2-10-F				10	1
Z-I-C (Control)			0	0	0
Z-A-0-1				1	0
Z-A-1-0	Zeolite	Isopropyl alcohol	1	0	0
Z-A-1-1				1	0
Z-A-2-0				0	0
Z-A-2-1			2	1	0
Z-DA-1-0				0	0
Z-DA-1-1	Zeolite	90% deionized water and 10% isopropyl alcohol	1	1	0
Z-DA-2-0				0	0
Z-DA-2-1				2	1
C-D-C (Control)	Coconut shell activated carbon	Deionized water	2	0	0
C-D-2-1				1	0
C-D-2-10				10	0
C-D-2-10-F				10	1

Note: the specimen notation includes five parts except for control specimens, which are Z-D-C, Z-I-C, and C-D-C; the first and second parts indicate the types of porous material and dilution solution for coating on the textile fabrics, the third part represents the ratio of the epoxy resin content in the dilution solution, and the fourth and fifth parts represent the number of washing and freeze–thaw cycles, respectively.

Figure 2 shows the coating method of zeolite or coconut shell activated carbon and the epoxy on the textile fibers. The considerably high viscosity of epoxy results in a high possibility of forming entangled lumps with the zeolite or coconut shell activated carbon powder [18]. Hence, to reduce the formation of entangled lumps, the epoxy needs to be diluted to a high-flow solution [19]. As shown in Figure 2, the deionized water or isopropyl alcohol for dilution was mixed with the epoxy resin for 3 min. Subsequently, the zeolite or coconut shell activated carbon powder was added and mixed for 5 min. The epoxy hardener was finally added and mixed for 2 min. The textile fibers were fully dipped into the combined dilution solution and stirred continuously. The dipping time was 30 min. The dipped textile fibers were dried under a shade at 20 ± 2 °C and $60\% \pm 2\%$ humidity.

Figure 3 shows the washing and freeze–thawing process of the textile fibers coated with porous materials. In the washing process, the textile fibers coated with porous materials were washed by running water with the water drop velocity of 3 m/s, which is the maximum water velocity in rain. In the freeze thawing process, the textile fibers were placed in a chamber with a temperature below -14 °C for 24 h after washing, and then thawed under the shade at 20 ± 2 °C and $60\% \pm 2\%$ humidity. Before testing, the processed textile fibers were dried under the shade.

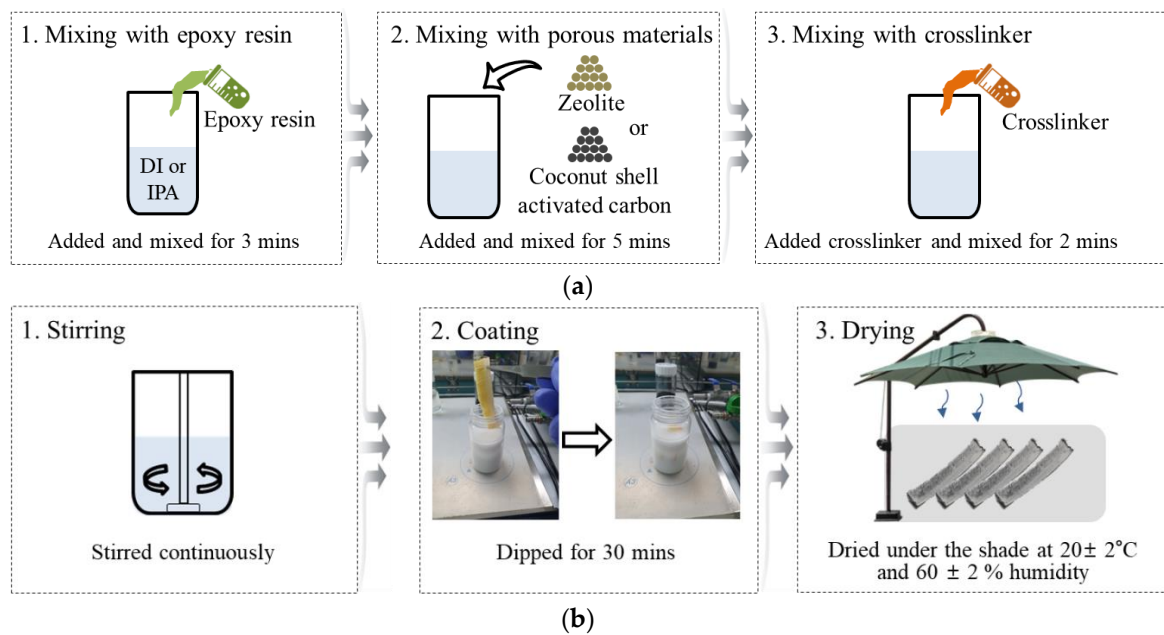


Figure 2. Coating method of the textile fabrics. (a) Producing dilution solution for coating. (b) Coating and drying.

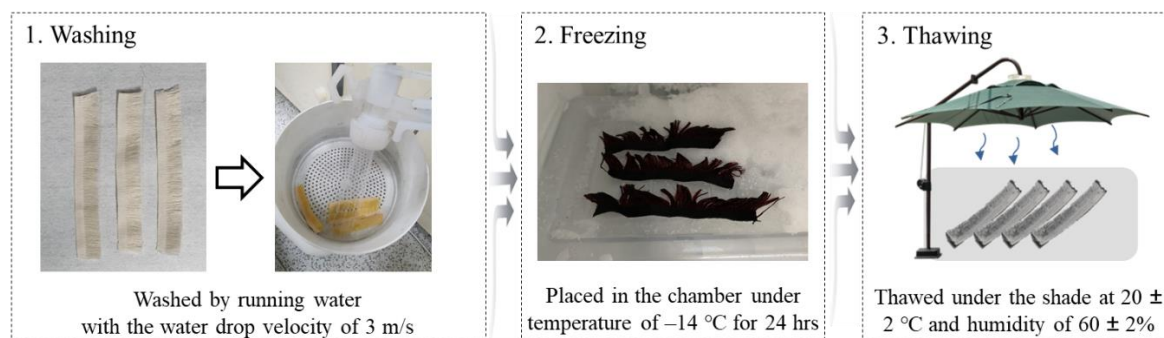


Figure 3. Washing and freeze–thaw process of the textile fabrics with porous materials.

The fine dust particles on the textile fibers were measured using a machine that counted the number of fine dust particles with a laser [20]. As shown in Figure 4a, the counting machine comprised a laser counter, a chamber, and a fan. The octagonal chamber had a dimension of $405\text{ mm} \times 405\text{ mm} \times 120\text{ mm}$. The dimension of the textile fabrics specimen was $115\text{ mm} \times 115\text{ mm} \times 10\text{ mm}$. The fabrics were attached onto plywood, which is not considerably affected by the static electricity, to fix it in the chamber (Figure 4b). To circulate the fine dust particles in the chamber, the fan was operated with a constant wind velocity of approximately 9.78 m/s during the experiment. The variation of the number of fine dust particles with respect to time was measured by counting the fine dust particles reflected by the laser. The fine dust particles used was A1 ultrafine test dust (ISO 12103-1, Arizona Test Dust), which is commonly used for the testing air purification filters [21]. The sizes of most of the A1 dust particles ranged between 0.97 and $5.5\ \mu\text{m}$, which is similar to that of the ultrafine dust particles ($2.5\ \text{PM}$) in the air [21]. Most of the A1 dust was circulated continuously by the airflow generated from the fan, whereas only some dust was attached to the chamber. Since the number of fine dust particles decreased even without the textile fibers in the chamber, the number of fine dust particles obtained from the chamber containing the textile fabric specimen was compared with that without the textile fabric specimen.

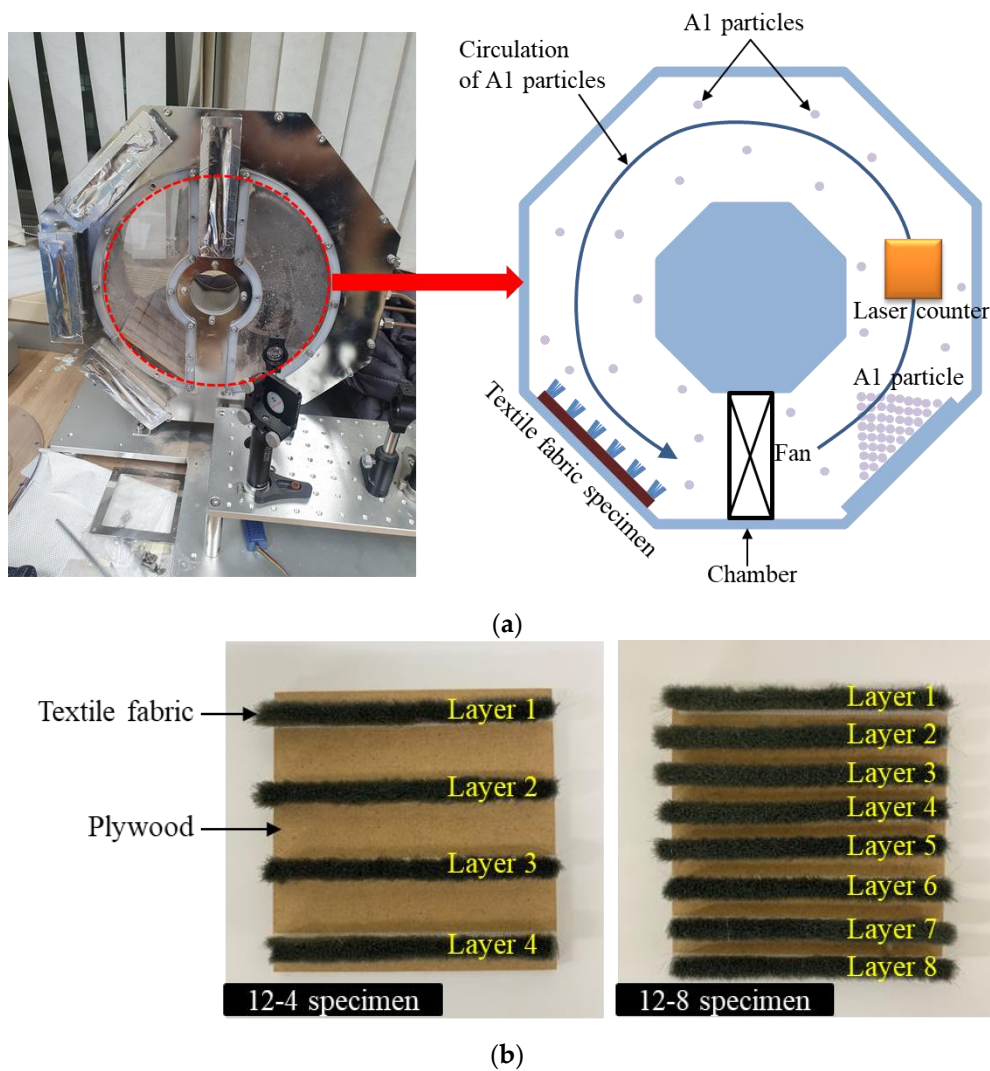


Figure 4. Test setup for measuring fine dust particle removal rates. (a) Schematic of machine for counting the fine dust particles. (b) Details of textile fabric specimens.

Figure 5 shows the measurement machine for the removal of SO_x and NO_x by the textile fabrics coated with the porous materials. The measurement machine was composed of a chamber, a velocity and flow controller, a gas inlet and outlet, and a gas analyzer. The chamber had shape of a rugby ball with a 90 mm inner diameter and 178 mm length. The textile fabric specimen was placed on the circular platform in the center of the chamber. SO_x or NO_x gas was then injected using the velocity and flow controller, and the decrease in the gas concentration in the chamber with the coated textile fabric specimen was measured using the gas analyzer connected to the gas outlet. The injection velocity and flow content were determined by the values required for maintaining a gas concentration of 1 ppm in the chamber without the specimen. The SO_x or NO_x removal rate of the coated textile fabric specimen was evaluated by comparing the variation of the gas concentration in the chamber with and without the specimen. In accordance with ISO 22197-1 [22], the SO_x or NO_x removal rate was calculated as follows:

$$R_{air} = \frac{D}{A_{REF}} \times 100 \quad (1)$$

where A_{REF} is the area under the graph of the variation of the gas concentration with respect to the time in the chamber, and D is the decrease in the graph area of the SO_x or NO_x concentration due to the specimen (Figure 6). The microstructures and compositions of the textile fabrics coated with

zeolite and coconut shell activated carbon were examined using SEM and energy dispersive X-ray spectroscopy (EDS) using an electron microscope.

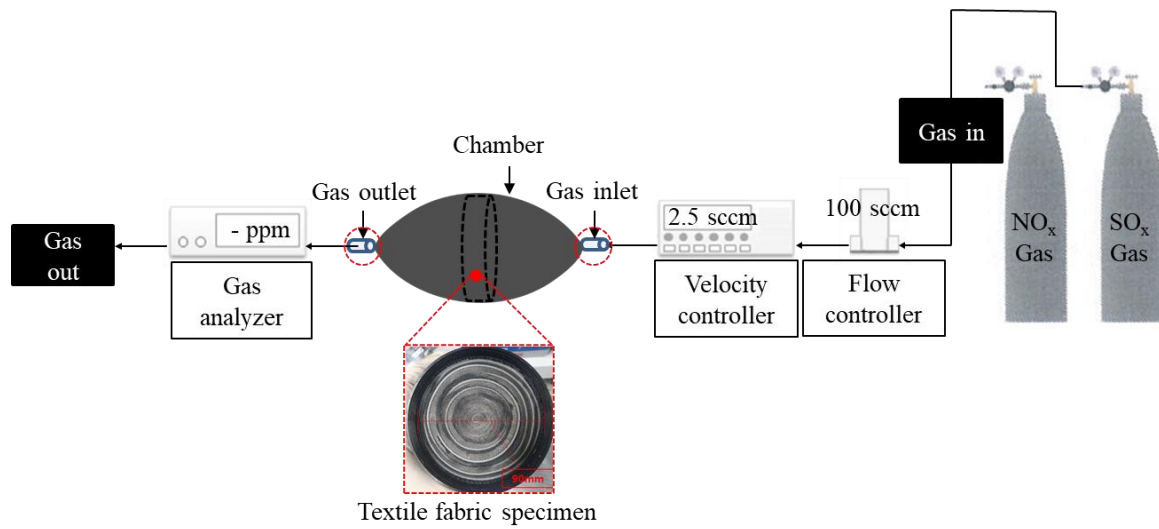


Figure 5. Machine for measuring SO_x and NO_x removal by the textile fabric.

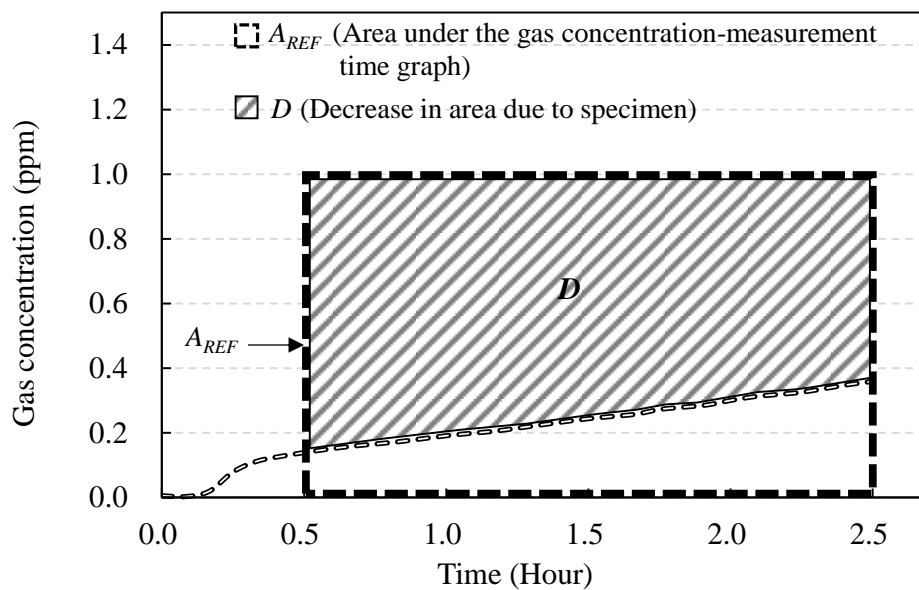


Figure 6. Variation of gas concentration with respect to time.

3. Results and Discussion

3.1. Effect of Length and Density of Textile Fabrics

Figure 7 shows the number of A1 particles with respect to the time. The decrease in the number of A1 particles obtained from the chamber without a specimen was less than 17% in the first 20 min. The decrease dramatically increased after that. The decrease at 30 min was approximately 78%. The point in time at which the decrease began to increase dramatically and the decrease became more notable occurred earlier as the length and density of the textile fabrics increased. The number of A1 particles dramatically decreased at 12 min for the specimen with 3.5 mm length and 4 layers, and at 7 min for the specimen with 12 mm length and 4 layers.

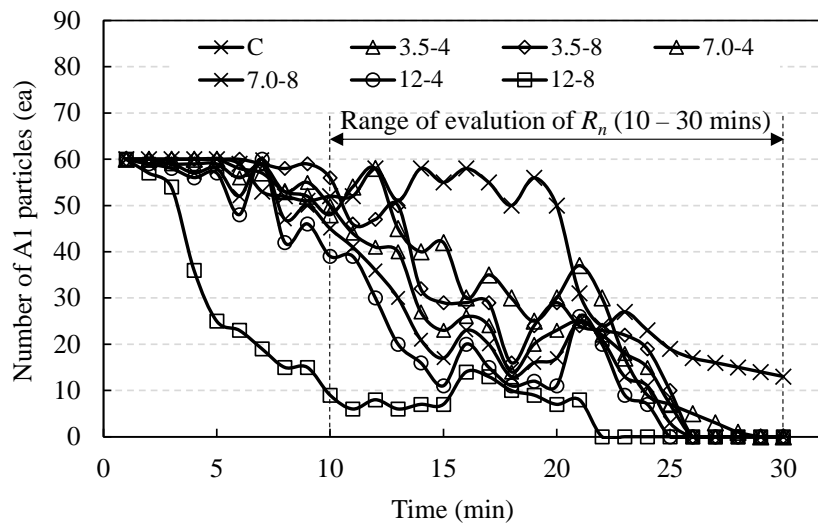


Figure 7. Number of A1 particles with respect to time.

The time at which the number of A1 particles reached zero was 29 min for the specimen with 3.5 mm length and 4 layers, and 26 min for the specimen with 3.5 mm length and 8 layers. The corresponding values were 25 min for the specimen with 12 mm length and 4 layers, and 22 min for the specimen with 12 mm length and 8 layers. Table 4 summarizes the results for the number of A1 particles. Due to the large scatter observed in the number of A1 particles with respect to time, the fine dust particle removal rate was evaluated by comparing the ratios (R_n) of the number of A1 particles obtained from the chamber with the specimen to that without the specimen between 10 and 30 min when the number of A1 particles decreased dramatically. The results are shown in Figure 7. At the end of the test, approximately 77.5% of the A1 particles were removed from the chamber without a specimen whereas all the particles were removed from the chamber with a specimen. Between 10 and 30 min, the R_n value increased with the length of the textile fibers, indicating that the increase was more notable for the specimens with denser textile fibers. The R_n of the specimen with 12 mm length and 4 layers was 1.8 times higher than that with 3.5 mm length and 4 layers. In addition, the R_n of the specimen with 12 mm length and 8 layers arrangement was 2.47 times higher than that with 3.5 mm length and 8 layers.

Table 4. Summary of the number of A1 particles adsorbed on the textile fabrics.

Specimens	Removal Rate of A1 Particles at Termination of Test (%)	Time which the Number of A1 Particles Reached Zero (min)	R_n (%)
C	77.5	-	-
3.5-4	100	29	20
3.5-8	100	26	21
7.0-4	100	26	23
7.0-8	100	25	33
12-4	100	25	36
12-8	100	22	52

R_n = The ratio of the number of A1 particles obtained from the chamber with specimen to that without a specimen between 10 and 30 min.

Figure 8 shows the SEM image and EDS spectra of the textile fibers before and after adsorbing the fine dust particles. Before adsorbing the fine dust particles, C and O were present at the proportions of 63.6% and 36.4%, respectively. After adsorbing the fine dust particles, the additional presence of 10.1% Si, 4.1% Al, and 3.3% K was observed. This implies that the definite adsorption of the fine dust particles on the surface of the textile fabrics because Si and Al were the main components of the fine dust particles. The adsorption of the fine dust particles was also confirmed from the SEM image.

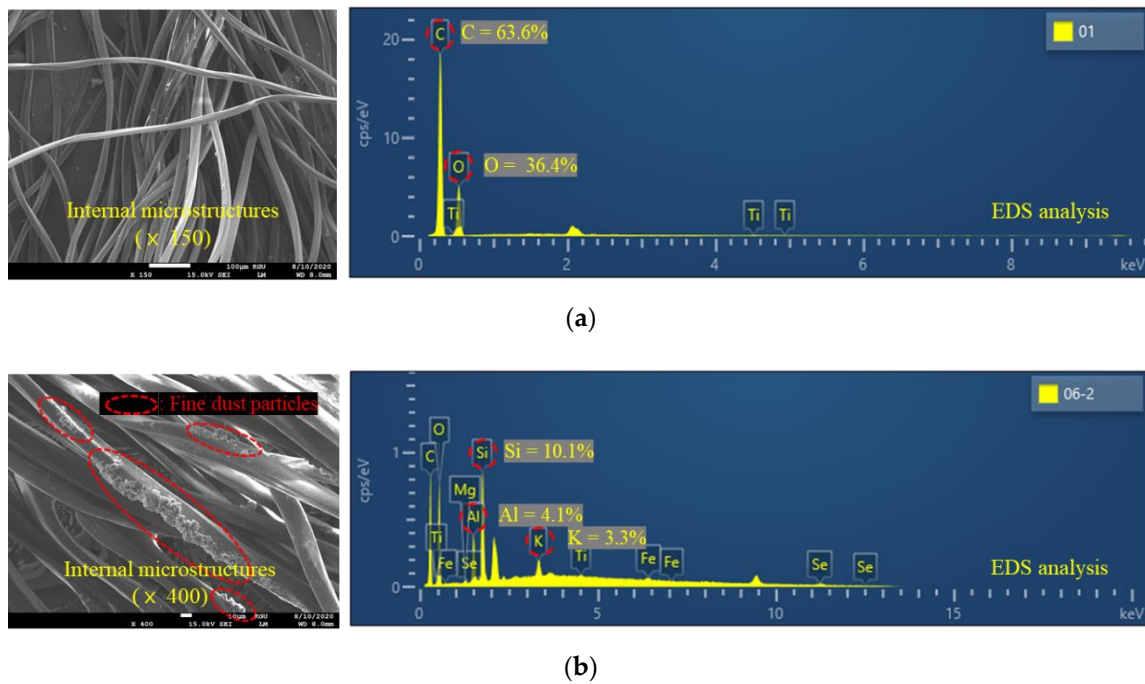


Figure 8. SEM images and EDS spectra of the uncoated textile fibers. (a) Before adsorption of the fine dust particles. (b) After adsorption of the fine dust particles.

3.2. Effect of Epoxy Content and Dilution Solution on SO_x Removal Rate

As summarized in Table 5, the SO_x removal rate decreased with the increase in the epoxy content, indicating that the decrease was affected by the solution type. The SO_x removal rate of the coated textile fabrics using deionized water as the dilution solution decreased by approximately 7% when the epoxy contents increased from 0 to 2%. The SO_x removal rate of the coated textile fibers using isopropyl alcohol as the dilution solution decreased by approximately 20%, which was approximately 2.8 times the decrease when deionized water was used as the dilution solution. In addition, the SO_x removal rate of the coated textile fibers using the combination of 90% deionized water and 10% isopropyl alcohol as the dilution solution decreased by approximately 8.9%, when the epoxy contents increased from 1 to 2%. This implies that the use of deionized water for the dilution solution was more effective for alleviating the decrease in the SO_x removal rate with the increase in epoxy contents than the use of isopropyl alcohol.

Table 5. Summary of the SO_x and NO_x removal rates of textile fabrics coated with zeolite or coconut shell activated carbon.

Specimens	Porous Material Type	Dilution Solution Type	Epoxy Contents (%)	Number of Washings	Number of Freezing-Thaw Cycles	Removal Rate (%)	
						SO _x	NO _x
Z-D-C (Control)			0	0	0	83.4	-
Z-D-0-1			0	1	0	34.9	-
Z-D-1-0			1	0	0	74.7	-
Z-D-1-1			1	1	0	66.2	-
Z-D-1.5-0	Zeolite	Deionized water	1.5	0	0	68.3	-
Z-D-1.5-1				1	0	60.8	-
Z-D-2-0				0	0	76.7	-
Z-D-2-1				1	0	77.2	-
Z-D-2-10				10	0	77.6	-
Z-D-2-10-F			2	10	1	75.5	-

Table 5. Cont.

Specimens	Porous Material Type	Dilution Solution Type	Epoxy Contents (%)	Number of Washings	Number of Freezing-Thaw Cycles	Removal Rate (%)	
						SO _x	NO _x
Z-I-C (Control)			0	0	0	86.3	-
Z-A-0-1	Zeolite	Isopropyl alcohol		1	0	26.6	-
Z-A-1-0			0	0	84.7	-	
Z-A-1-1			1	0	58.8	-	
Z-A-2-0			2	0	66.1	-	
Z-A-2-1			1	0	62.4	-	
Z-DA-1-0	Zeolite	90% deionized water and 10% isopropyl alcohol		0	0	90.6	-
Z-DA-1-1			1	0	73.4	-	
Z-DA-2-0			0	0	81.7	-	
Z-DA-2-1			2	0	74.8	-	
C-D-C (Control)	Coconut shell activated carbon	Deionized water		0	0	-	19.8
C-D-2-1			2	1	0	-	16.9
C-D-2-10				10	0	-	16.6
C-D-2-10-F				10	1	-	16.3

3.3. Effect of the External Environment on SO_x Removal Rate

Figure 9 shows the SO_x removal rate of the textile fibers coated with zeolite after exposure to the external environment. After one washing, the SO_x removal rate dramatically decreased. The decrease was 52.5% at 2% epoxy content. The lowest SO_x removal rate in the textile fibers using deionized water as the dilution solution was 34.9% at the epoxy content of 0%. The removal rate was 77.2% at the epoxy content of 2%, which was 2.2 times higher than that at the epoxy content of 0%. After 10 washings, the SO_x removal rate of the coated textile fibers using deionized water as the dilution solution was 77.6% at 2% epoxy content. In addition, after 10 washings and a single freeze–thaw cycle. The removal rate was 75.5%, which was similar to that before exposure to the external environmental conditions of washing and freeze thawing. Meanwhile, the SO_x removal rate of the coated textile fibers using isopropyl alcohol as the dilution solution after one washing exhibited similar trends to the removal rate using deionized water as the dilution solution. After one washing, the SO_x removal rate of the coated textile fibers using isopropyl alcohol as the dilution solution was 26.6% at the epoxy content of 0%, and 62.4% at the epoxy content of 2%. This implies that a higher epoxy content is effective in maintaining a stable SO_x removal rate in external environmental conditions such as washing or freeze thawing, because the epoxy directly affected the degree of adhesion between the textile fabrics and the zeolite.

Figure 10 shows the SEM image and EDS spectra of the textile fabrics coated with zeolite. As shown in Figure 10a, before washing, O and Ca, which were the main components of zeolite, were present in the coated fabric in the proportions of 36.7% and 18.1%, respectively. After 10 washings and one freeze–thaw cycle, the proportions of O and Ca were 38.5% and 5.8%, respectively. This implies that the zeolite was well attached to the surface of the textile fabrics after exposure to external environmental condition such as washing or freeze thawing. The attachment of the zeolite to the fabrics was also confirmed in the SEM image in Figure 10b.

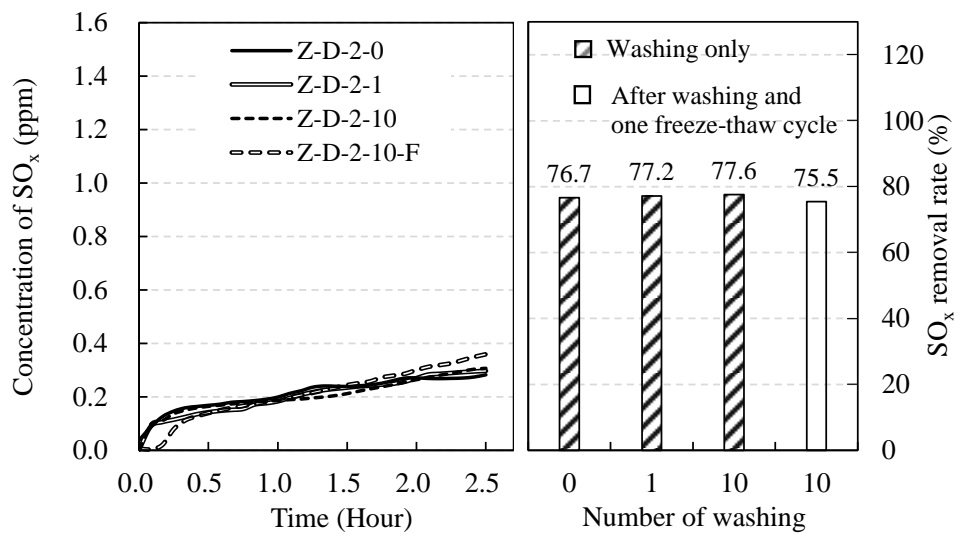


Figure 9. Typical SO_x removal rate of textile fabrics coated with zeolite after exposure to external environmental conditions.

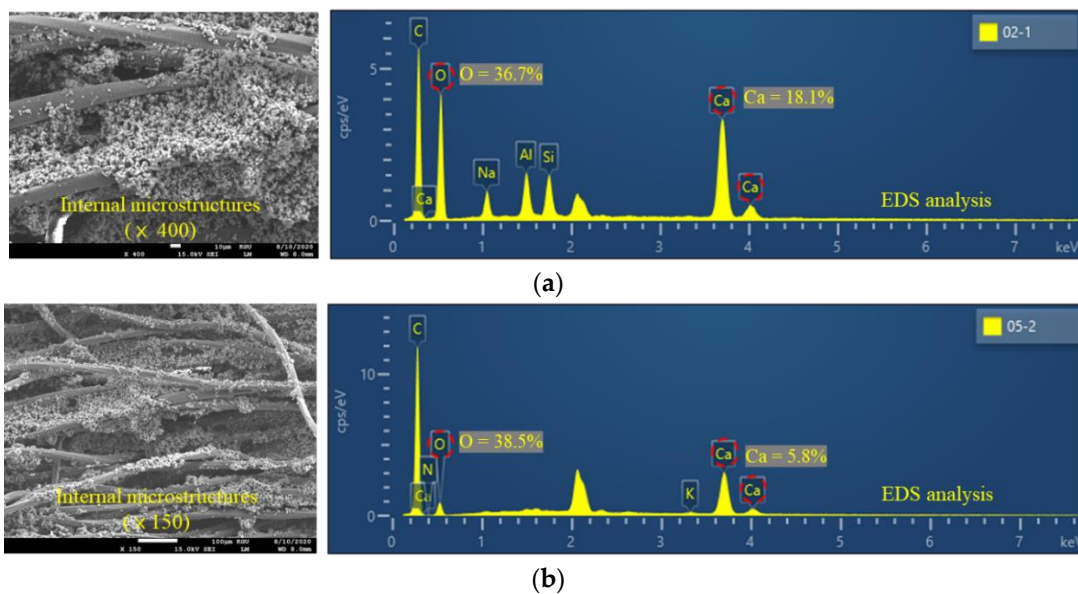


Figure 10. SEM images and EDS spectra of textile fabric coated with zeolite. (a) Before washing. (b) After 10 washings and one freeze–thaw cycle.

3.4. Effect of External Environment Condition on the NO_x Removal Rate

Based on the results obtained from Sections 3.2 and 3.3, the textile fibers were coated with coconut shell activated carbon using 98% deionized water for the dilution solution and 2% epoxy. Figure 11 shows the NO_x removal rate of the textile fibers coated with coconut shell activated carbon after exposure to external environmental conditions. The washing and freeze thawing procedures were identical to those in Section 3.3. Before washing, the NO_x removal rate was 19.8%. This value was maintained after one and after 10 washings in which the removal rates were 16.9% and 16.6%, respectively. In particular, after 10 washings and one freeze–thaw cycle, the NO_x removal rate was 16.3%, which was similar to that after one washing. This implies that the coating conditions of the solution type and epoxy content determined from the coating procedure of textile fibers with zeolite were effective in maintaining a stable NO_x removal rate in textile fibers coated with coconut shell activated carbon in external environments.

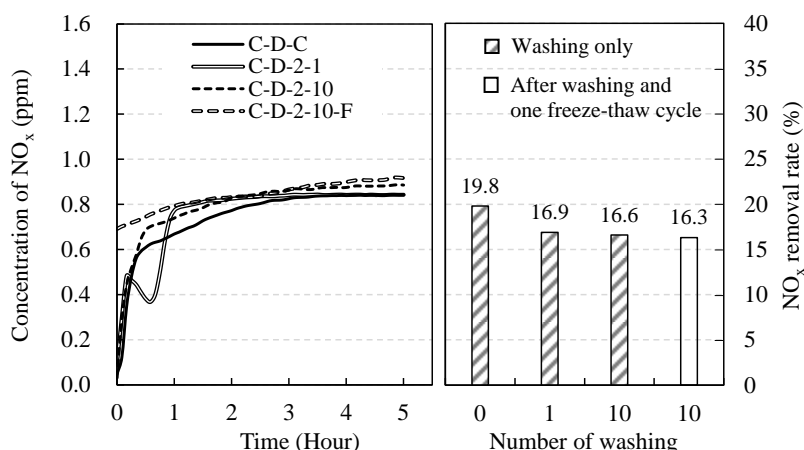


Figure 11. NO_x removal rate of textile fabrics coated with coconut shell activated carbon after exposure to external environmental conditions.

Figure 12 shows the SEM image and EDS spectra of the textile fibers coated with coconut shell activated carbon. As shown in Figure 12a, before washing, C, which is the main components of coconut shell activated carbon, was present at the proportion of 84.7%. After 10 washings and one freeze–thaw cycle, the proportion of C was 99.9%. This implies that the coconut shell activated carbon was well attached to the surface of the textile fabrics after exposure to external environmental conditions such as washing or freeze thawing. The attachment of the coconut shell activated carbon was also confirmed in the SEM image in Figure 12b.

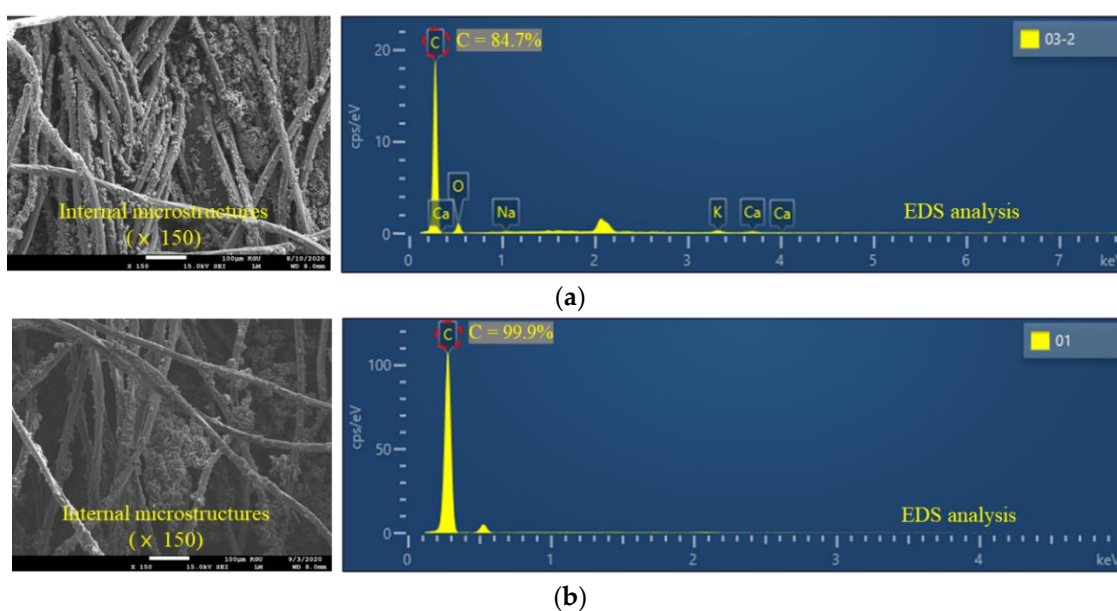


Figure 12. SEM images and EDS spectra of the uncoated textile fibers. (a) Before washing. (b) After 10 washings and one freeze–thaw cycle.

4. Conclusions

An effective method for coating textile fabrics with porous materials was proposed by using the optimum conditions for an epoxy solution, which was mixed with a resin, crosslinker, and dilution solution. The removal rate of fine dust particles in uncoated textile fabrics increased by 1.8 and 2.47 times for textile fibers with 4 and 8 layers, respectively, when the length of the textile fabric increased from 2.5 to 12 mm. The sulfur oxides (SO_x) removal rate of the textile fabrics coated with zeolite decreased with the increase in the epoxy content ratio. The decrease in the textile fabrics using

isopropyl alcohol as the dilution solution was 23.4%, which was 2.9 times higher than in the textile fabrics using deionized water as the dilution solution. After one washing, the textile fabrics coated with zeolite without using epoxy had the lowest SO_x removal rate of 26.6%, whereas the corresponding values using an epoxy content of 2% and deionized water or isopropyl alcohol for the dilution solution were 77.2% and 62.4%, respectively, which were similar to the values before washing. After 10 washings and one freeze–thaw cycle, the SO_x and nitrogen oxides (NO_x) removal rates of the coated textile fibers using deionized water and the epoxy contents of 2% were 75.5% and 16.3%, respectively, similar to those after one washing. In the coated textile fibers before washing or freeze thawing, the proportions of O and C, which were the main components of zeolite and coconut shell activated carbon, were 36.7% and 84.7%, respectively. These values were similar to those for the coated textile fibers exposed to 10 washings and one freeze–thaw cycle. Consequently, to maintain stable SO_x and NO_x removal rates in the textile fabrics exposed to external environmental conditions such as washing and freeze thawing, 98% deionized water for the dilution solution and 2% epoxy content were required for the optimum coating of the textile fibers with zeolite and coconut shell activated carbon.

Author Contributions: K.-H.Y. designed project. J.-H.M. and J.-U.L. conducted the analysis of test results obtained this study. All authors contributed to the comprehensive analysis and conclusion. All authors have read and agreed to the published version of the manuscript.

Funding: This research was funded by the Korea Institute of Energy Technology Evaluation and Planning (KETEP) and the Ministry of Trade, Industry & Energy (MOTIE) of the Republic of Korea.

Acknowledgments: This work was supported by the Korea Institute of Energy Technology Evaluation and Planning (KETEP) and the Ministry of Trade, Industry & Energy (MOTIE) of the Republic of Korea (No. 20181110200070).

Conflicts of Interest: The authors declare no conflict of interest.

References

1. Jiang, K.; Yu, H.; Chen, L.; Fang, M.; Azzi, M. An advanced, ammonia-based combined NO_x/SO_x/CO₂ emission control process towards a low-cost, clean coal technology. *Appl. Energy* **2020**, *260*, 114316. [[CrossRef](#)]
2. Yu, H.; Morgan, S.; Allport, A.; Do, T.; Cottrell, A.; McGregor, J. Update on aqueous ammonia based post combustion capture pilot plant at Munmorah. *Distill. Absorpt.* **2010**, *NL*, 115–120.
3. Trapalis, A.; Todorova, N.; Giannakopoulou, T.; Boukos, N.; Speliotis, T.; Dimotikali, D.; Yu, J. TiO₂/graphene composite photocatalysts for NO_x removal: A comparison of surfactant-stabilized graphene and reduced graphene oxide. *Appl. Catal. B Environ.* **2016**, *180*, 637–647. [[CrossRef](#)]
4. Guo, M.Z.; Ling, T.C.; Poon, C.S. Photocatalytic NO_x degradation of concrete surface layers intermixed and spray-coated with nano-TiO₂: Influence of experimental factors. *Cem. Concr. Compos.* **2017**, *83*, 279–289. [[CrossRef](#)]
5. Dylla, H.; Hassan, M.M.; Schmitt, M.; Rupnow, T.; Mohammad, L.M. Laboratory investigation of the effect of mixed nitrogen dioxide and nitrogen oxide gases on titanium dioxide photocatalytic efficiency in concrete pavements. *J. Mater. Civ. Eng.* **2010**, *23*, 1087–1093. [[CrossRef](#)]
6. Yoon, I.H.; Lee, K.B.; Kim, J.S.; Kim, S.D. A study on the estimation of NO_x reduction in ambient by photocatalyst (TiO₂) block. *J. Korean Soc. Urban Environ.* **2017**, *17*, 433–443.
7. An, E.J. A study of dyeing polyester fiber using alkali treatment. *J. Basic Des. Art* **2014**, *15*, 185–194.
8. Kim, K.T.; Ahn, Y.C.; Lee, J.K. Characteristic analysis of electret filters made by electrospinning. *Korean J. Air Cond. Refrig. Eng.* **2008**, *20*, 820–824.
9. Wang, Z.; Guo, M.; Mu, X.; Sen, S.; Insley, T.; Mason, A.J.; Král, P.; Zeng, X. Highly sensitive capacitive gas sensing at ionic liquid–electrode. *Anal. Chem.* **2016**, *88*, 1959–1964. [[CrossRef](#)] [[PubMed](#)]
10. Kopaq, T.; Kaymakgi, E.; Kopac, M. Dynamic adsorption of SO₂ on zeolite molecular sieves. *Chem. Eng. Commun.* **1998**, *164*, 99–109. [[CrossRef](#)]
11. Lee, S.J.; Shin, C.S.; Lee, T.H. Removal and regeneration of SO₂ by cupric oxide supported on zeolite. *J. Korean Soc. Atmos. Environ.* **1990**, *6*, 161–167.
12. Kopaç, T.; Kocabaş, S. Sulfur dioxide adsorption isotherms and breakthrough analysis on molecular sieve 5A zeolite. *Chem. Eng. Commun.* **2010**, *190*, 1041–1054. [[CrossRef](#)]

13. Chiang, Y.C.; Chiang, P.C.; Chang, E.E. Effects of surface characteristics of activated carbons on VOC adsorption. *J. Environ. Eng.* **2001**, *127*, 54–62. [[CrossRef](#)]
14. Al-Rahbi, A.S.; Williams, P.T. Production of activated carbons from waste tyres for low temperature NO_x control. *Waste Manag.* **2016**, *49*, 188–195. [[CrossRef](#)] [[PubMed](#)]
15. Park, S.J.; Kim, B.J.; Kawasaki, J. NO removal of electrolessly copper-plated activated carbons. *Hwahak Konghak* **2003**, *41*, 795–801.
16. Lee, S.W.; Bae, S.K.; Kwon, J.H.; Na, Y.S.; An, C.D.; Yoon, Y.S.; Song, S.K. Correlations between pore structure of activated carbon and adsorption characteristics of acetone vapor. *Korean Soc. Environ. Eng.* **2005**, *27*, 620–625.
17. Lim, T.K.; Lee, J.H.; Mun, J.H.; Yang, K.H.; Ju, S.H.; Jeong, S.M. Enhancing functionality of epoxy-TiO₂-embedded high-strength lightweight aggregates. *Polymers* **2020**, *12*, 2384. [[CrossRef](#)] [[PubMed](#)]
18. Zhang, D.; Jia, D. Toughness and strength improvement of diglycidyl ether of bisphenol-A by low viscosity liquid hyperbranched epoxy resin. *J. Appl. Polym. Sci.* **2006**, *101*, 2504–2511. [[CrossRef](#)]
19. Varley, R.J. Toughening of epoxy resin systems using low-viscosity additives. *Polym. Int.* **2004**, *53*, 78–84. [[CrossRef](#)]
20. Bong, C.K.; Kim, Y.G.; Lee, J.H.; Bong, H.K.; Kim, D.S. Mutual comparison between two the real-time optical particle counter for measuring fine particles. *J. Korean Soc. Urban Environ.* **2015**, *15*, 219–226.
21. ISO 12103-1. *Road Vehicles-Test Dust for Filter Evaluation—Part 1: Arizona Test Dust*; International Organization for Standardization: Geneva, Switzerland, 1997.
22. ISO 22197-1. *Fine Ceramics (Advanced Ceramics, Advanced Technical Ceramics)—Test Method for Air-Purification Performance of Semiconducting Photocatalytic Materials—Part 1: Removal of Nitric Oxide*; International Organization for Standardization: Geneva, Switzerland, 2007.

Publisher's Note: MDPI stays neutral with regard to jurisdictional claims in published maps and institutional affiliations.



© 2020 by the authors. Licensee MDPI, Basel, Switzerland. This article is an open access article distributed under the terms and conditions of the Creative Commons Attribution (CC BY) license (<http://creativecommons.org/licenses/by/4.0/>).